12th International Conference on Applications of Statistics and Probability in Civil Engineering, ICASP12
Vancouver, Canada, July 12-15, 2015

Fusing Simulation Results From Multifidelity Aero-servo-elastic Simulators - Application To Extreme Loads On Wind Turbine

Imad Abdallah
Technical University of Denmark, Department of Wind Energy, Roskilde, Denmark

Bruno Sudret
ETH Zürich, Chair of Risk, Safety and Uncertainty Quantification, Zürich, Switzerland

Christos Lataniotis
ETH Zürich, Chair of Risk, Safety and Uncertainty Quantification, Zürich, Switzerland

John D. Sørensen
Aalborg University, Department of Civil Engineering, Aalborg, Denmark

Anand Natarajan
Technical University of Denmark, Department of Wind Energy, Roskilde, Denmark

ABSTRACT: Fusing predictions from multiple simulators in the early stages of the conceptual design of a wind turbine results in reduction in model uncertainty and risk mitigation. Aero-servo-elastic is a term that refers to the coupling of wind inflow, aerodynamics, structural dynamics and controls. Fusing the response data from multiple aero-servo-elastic simulators could provide better predictive ability than using any single simulator. The co-Kriging approach to fuse information from multifidelity aero-servo-elastic simulators is presented. We illustrate the co-Kriging approach to fuse the extreme flapwise bending moment at the blade root of a large wind turbine as a function of wind speed, turbulence and shear exponent in the presence of model uncertainty and non-stationary noise in the output. The extreme responses are obtained by two widely accepted numerical aero-servo-elastic simulators, FAST and BLADED. With limited high-fidelity response samples, the co-Kriging model produced notably accurate prediction of validation data.

1. INTRODUCTION

Analysts and designers increasingly use multiple commercial and research-based aero-servo-elastic simulators to compare the prediction of wind turbines' structural response. The aero-servo-elastic simulators are of varying fidelity and have different underlying assumptions. As a result, the aero-servo-elastic response may vary amongst simulators even if the external inflow condition is the same. The sub-models with the largest impact on the aero-servo-elastic response variability are aerodynamic, structural, control systems and wind inflow. The aero-servo-elastic simulators are validated using test measurements from prototype wind turbines. The current practice is to cover the discrepancy amongst the simulators by imposing safety factors resulting in a safe design. It is reasonable to assume that model uncertainty is of the epistemic type and can be estimated at the design stage with (usually) decreasing uncertainty when more simulations from multiple sources are available.

The objective in this paper is to fuse the extreme response from multiple aero-servo-elastic simulators of various fidelity and complexity to predict "the most likely" extreme response of a wind turbine. Forrester et al. (2007) used the co-Kriging technique in the optimization of a generic aircraft wing using one "cheap" and one "expensive" flow solver. The Co-Kriging approach was also used by

Han and Görtz (2012) to predict the mean aerodynamic lift and drag coefficients on a two dimensional airfoil and a three dimensional aircraft using a low-fidelity Euler flow solver and a high-fidelity Navier-Stokes solver.

The novelty in this paper is the implementation of the co-Kriging technique to predict the extreme (not the mean) response in the presence of non-stationary noise in the output (i.e. the magnitude of noise varies as a function of the input variables) in the case when the low and high-fidelity aero-servo-elastic simulators of the same wind turbine are implemented by two independent engineers (i.e. human error and uncertainty in the modelling and input assumptions are implicitly included). In this paper, we demonstrate the co-Kriging methodology to fuse the extreme blade root flapwise bending moment of a large multi-megawatt wind turbine by using two aero-servo-elastic simulators, FAST (Jonkman and Buhl, 2005) and BLADED (Bossanyi (2003a), Bossanyi (2003b)).

2. THE CASE FOR DATA FUSION

Wind turbine aero-servo-elastic simulators of varying fidelities exhibit similarities and dependence in terms of the input variables and the underlying physical models (aerodynamic, structural, control systems and wind inflow). The dependence amongst various simulators may not be quantified by a single scalar number; it may well be that the dependence varies as a function of the design and input space (Christensen, 2012). Thus, we ask the fundamental question: Does it make any sense to fuse information from multifidelity aero-servo-elastic simulators $\mathscr{M}_i$?

- To a great extent, simulators $\{\mathscr{M}_i$, i=1,...,n$\}$ share similar (often identical) inputs and describe similar (often identical) underlying modelling and physics assumptions.
- The various simulators may have been calibrated using the same test measurements.
- The higher fidelity simulators may simply be an expansion of the lower fidelity simulation model by inclusion of additional physics.
- Let us assume that for a given set of inputs $\mathscr{X} = [\boldsymbol{x}^{(1)},...,\boldsymbol{x}^{(N)}]$, simulators $\mathscr{M}_i$ predict responses $\mathscr{Y}_i = [\mathscr{M}_1(\boldsymbol{x}^{(1)}),...,\mathscr{M}_i(\boldsymbol{x}^{(N)})]^T$. Then, $\mathscr{Y}_i$ generally share the same trend and do not differ significantly from each other. In addition, the simulators $\mathscr{M}_i$ do not exhibit clear bias in the predicted response $\mathscr{Y}_i$.
- The various aero-servo-elastic simulators may have been coded by the same or cooperating engineers, scientists and research institutes, and the same experts may have given their inputs/reviews/recommendations during the development and validation of the various simulators $\mathscr{M}_i$ resulting in similar assumptions and biases being used.
- The various simulators $\mathscr{M}_i$ are certified by accredited institutes for use in the industry to design wind turbines. The certification process involves a lengthy validation and verification against measurements. Hence, no particular simulator $\mathscr{M}_i$ is deemed better than the other.

The implication of the argumentation above is that rather than treating the aero-servo-elastic numerical simulators as parts of a hierarchy, they are considered as individual (but correlated) information sources. Furthermore, the simulators are assumed to be black boxes and we focus on the output quantity of interest (response) $\mathscr{Y}_i$.

3. METHODOLOGY

3.1. Co-Kriging

In this section we present a brief theoretical description of Kriging and Co-Kriging based on work by Sacks et al. (1989), Kennedy and O'Hagan (2000), Jones (2001), Forrester et al. (2007), Dubourg (2011), Han et al. (2012) , Picheny et al. (2012), Sudret (2012) and Schöbi and Sudret (2014). Kriging is a stochastic interpolation technique which assumes that the "true" model output is a realization of a Gaussian process:

$$Y(x) = \mu(x) + Z(x) \tag{1}$$

where $\mu(x)$ is the mean value of the Gaussian process (trend) and $Z(x)$ is a zero-mean stationary Gaussian process with variance σ_Y^2 and a Covariance of the form:

$$C(\boldsymbol{x},\boldsymbol{x}') = \sigma_Y^2 R\left(\boldsymbol{x}-\boldsymbol{x}' \mid \boldsymbol{\theta}\right) \tag{2}$$

where $\boldsymbol{\theta}$ gathers the hyperparameters of the autocorrelation function R. From a design of experiments $\mathscr{X}$, one can build the correlation matrix with terms $\boldsymbol{R}_{ij} = R\left(\boldsymbol{x}^{(i)}, \boldsymbol{x}^{(j)} \mid \boldsymbol{\theta}\right)$ representing the correlation between the sampled (observed) points. In the case of simple Kriging $\mu(x)$ is assumed to be a known constant. In the case of ordinary Kriging $\mu(x)$ is assumed to be an unknown constant. In the case of universal Kriging $\mu(x)$ is cast as $\sum_{j=0}^{m} \beta_j f_j(x)$, i.e. a linear combination of unknown (to be determined) linear regression coefficients $\beta_j, j = 1, ..., m$ and a set of preselected basis functions $f_j(x), j = 1, ..., m$ (usually predefined polynomial functions). The autocorrelation function R may be a generalized exponential kernel:

$$R(\boldsymbol{x}, \boldsymbol{x}') = \exp\left(-\sum_{i=1}^{M} \theta_i (\boldsymbol{x}_i - \boldsymbol{x}'_i)^{p_i}\right), \theta_i \geq 0, p_i \in (0, 2] \tag{3}$$

where M is the number of dimensions of the input space and θ_i and p_i are unknown parameters to be determined. Other choices for R is a Gaussian kernel, or a Matérn kernel, etc. In order to establish a Kriging surrogate model, a design of experiments is formed $\mathscr{X} = [\boldsymbol{x}^{(1)}, ..., \boldsymbol{x}^{(N)}]$ and a corresponding set of computer simulations are performed. The output is gathered in a vector $\mathscr{Y} = [\mathscr{M}(\boldsymbol{x}^{(1)}), ..., \mathscr{M}(\boldsymbol{x}^{(N)})]^T$. The Kriging estimator (predicted response given the design of experiments) at a new point $\boldsymbol{x}^* \in \mathscr{D}_X$ is a Gaussian variable $\hat{Y}(\boldsymbol{x}^*)$ with mean $\mu_{\hat{Y}}$ and variance $\sigma^2_{\hat{Y}}$ defined as (Best Linear Unbiased Estimator):

$$\begin{aligned} \mu_{\hat{Y}}(\boldsymbol{x}^*) &= \mathbb{E}\left[\hat{Y}(\boldsymbol{x}^*) \mid \mathscr{M}\left(\boldsymbol{x}^{(i)}\right)\right] \\ &= \boldsymbol{f}^T \hat{\boldsymbol{\beta}} + \boldsymbol{r}^T \boldsymbol{R}^{-1}\left(\mathscr{Y} - \boldsymbol{F}\hat{\boldsymbol{\beta}}\right) \end{aligned} \tag{4}$$

$$\begin{aligned} \sigma^2_{\hat{Y}}(\boldsymbol{x}^*) &= \mathrm{Var}\left[\hat{Y}(\boldsymbol{x}^*) \mid \mathscr{M}\left(\boldsymbol{x}^{(i)}\right)\right] \\ &= \hat{\sigma}^2_Y\left[1 - \boldsymbol{r}^T \boldsymbol{R}^{-1} \boldsymbol{r} + \boldsymbol{u}^T (\boldsymbol{F}^T \boldsymbol{R}^{-1} \boldsymbol{F})^{-1} \boldsymbol{u}\right] \end{aligned} \tag{5}$$

where the optimal Kriging variance $\hat{\sigma}^2_Y$ and optimal Kriging trend coefficients $\hat{\boldsymbol{\beta}}(\boldsymbol{\theta})$ are given by:

$$\hat{\sigma}^2_Y = \frac{(\mathscr{Y} - \boldsymbol{F}\hat{\boldsymbol{\beta}})^T \boldsymbol{R}^{-1} (\mathscr{Y} - \boldsymbol{F}\hat{\boldsymbol{\beta}})}{N} \tag{6}$$

$$\hat{\boldsymbol{\beta}} = \left(\boldsymbol{F}^T \boldsymbol{R}^{-1} \boldsymbol{F}\right)^{-1} \boldsymbol{F}^T \boldsymbol{R}^{-1} \mathscr{Y} \tag{7}$$

and $\boldsymbol{u}$, $\boldsymbol{r}$ and $\boldsymbol{F}$ are given by:

$$\boldsymbol{u} = \boldsymbol{F}^T \boldsymbol{R}^{-1} \boldsymbol{r} - \boldsymbol{f} \tag{8}$$

$$\boldsymbol{r} = \begin{bmatrix} R(\boldsymbol{x}^* - \boldsymbol{x}^{(1)}; \hat{\boldsymbol{\theta}}) \\ \vdots \\ R(\boldsymbol{x}^* - \boldsymbol{x}^{(N)}; \hat{\boldsymbol{\theta}}) \end{bmatrix} \tag{9}$$

$$\boldsymbol{F} = \left[f_j(\boldsymbol{x}^{(i)})\right] = \begin{bmatrix} f_0(\boldsymbol{x}^{(1)}) & \dots & f_m(\boldsymbol{x}^{(1)}) \\ \vdots & & \\ f_0(\boldsymbol{x}^{(N)}) & \dots & f_m(\boldsymbol{x}^{(N)}) \end{bmatrix} \tag{10}$$

Note that $\boldsymbol{r}$ is the correlation matrix between the sampled points and the point where a prediction is to be made. In the general case of a-priori unknown correlation parameters $\hat{\boldsymbol{\theta}}$, the optimal values can be estimated through Bayesian inference, maximum likelihood estimate or a leave-one-out cross-validation (Bachoc, 2013).

In case the outputs of the computer experiments contain "noise", the Kriging model should regress the data in order to generate a smooth trend. The Kriging thus amounts to conditioning $\hat{Y}(\boldsymbol{x}^*)$ on noisy observations $\mathscr{M}\left(\boldsymbol{x}^{(i)}\right) + \varepsilon_i$. The Kriging estimator mean $\mu_{\hat{Y}}(\boldsymbol{x}^*)$ and variance $\sigma^2_{\hat{Y}}(\boldsymbol{x}^*)$ are given by Equations 4 and 5, respectively by replacing the correlation matrix $\boldsymbol{R}$ with $\boldsymbol{R} + \lambda^2 \boldsymbol{I}$, where λ^2 is the estimated variance of the noise term ε_i. We now consider how to build a surrogate model of a highly complex and expensive-to-run aero-servo-elastic response that is enhanced with data from cheaper and approximate analyses. This approach is traditionally known as co-Kriging (Kennedy and O'Hagan, 2000). Co-Kriging has been proposed under various names such as "hierarchical Kriging", "multifidelity surrogate modelling", "variable fidelity surrogate modelling", "data fusion", "multi-stage surrogate modelling", "recursive co-Kriging", etc. The formulation of co-Kriging presented here is based on Han and Görtz (2012): we consider l sets of response data obtained by running l aero-servo-elastic numerical simulators of varying fidelity and computational expense. We denote by level s the response data of the highest level of fidelity. For any given level $1 \leq l \leq s$, co-Kriging can

be written as:

$$\mu_{\hat{Y}}^{(l)} = \hat{\boldsymbol{\beta}}\mu_{\hat{Y}}^{(l-1)} + \boldsymbol{r}^T\boldsymbol{R}^{-1}(\mathscr{Y} - \boldsymbol{F}\hat{\boldsymbol{\beta}}) \qquad (11)$$

where $\hat{\boldsymbol{\beta}}$ is a scaling factor with a similar expression as in Equation 7, indicating how much the low- and high-fidelity responses are correlated to each other. $\mu_{\hat{Y}}^{(l-1)}$ is the trend in the kriging of the data at level l and the expression $\boldsymbol{R}^{-1}(\mathscr{Y} - \boldsymbol{F}\hat{\boldsymbol{\beta}})$ depends only on the sampled data at level l. An appealing feature of the above formulation is that it entails very little modifications to an existing Kriging code if the latter is sufficiently modular.

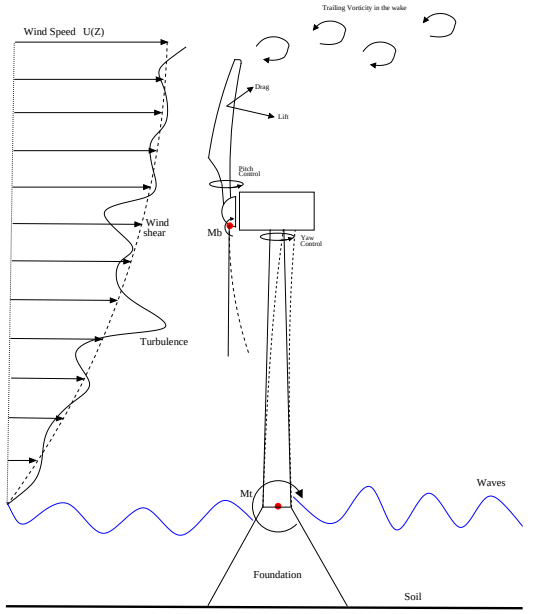

Figure 1: A wind turbine. M_b is the flapwise bending moment at the blade root. $U(Z)$ is the mean wind speed at height Z. Verical wind shear (dotted grey line) and turbulence (thick black line).

4. APPLICATION TO EXTREME LOADS ON WIND TURBINE

We illustrate co-Kriging in fusing the extreme flapwise bending moment at the blade root of a wind turbine (Figure 1) by using two numerical aero-servo-elastic simulators, FAST and BLADED.

4.1. Aero-servo-elastic simulations

FAST is a time-domain aero-servo-elastic simulator that employs a combined modal and multibody dynamics formulation. FAST models the turbine using 24 Degrees of Freedom (DOFs). These DOFs include two blade-flap modes and one blade-edge mode per blade. It has two fore-aft and two side-to-side tower bending modes in addition to nacelle yaw. The other DOFs represent the generator azimuth angle and the compliance in the drive train between the generator and hub/rotor. The aerodynamic model is based on the Blade Element Momentum theory (Hansen, 2001). A design of experiments (Table 1) is produced in order to examine the effects of wind speed, inflow turbulence and shear variations on the predicted extreme loads. For each combination of wind speed, turbulence level and shear exponent we generate realizations of wind time series with 24 stochastic seeds. Some of the wind speed, turbulence and shear exponent combinations are excluded because they are unphysical, resulting in a total of 33,480 10-minute time series simulations. One 10-minute wind time series simulation in FAST takes approximately three minutes in real time. The output used from the simulations are the blade root flapwise bending moment. The global maxima of the bending moment data are extracted for each of the 33,480 10-minute time series.

Table 1: Design of experiments for the FAST simulations. The variables are wind speed [m/s], turbulence [m/s] and the wind shear exponent.

Wind Speed [m/s]	Turbulence [m/s]	Shear exponent [-]
$4, 5, \cdots, 25$	0.1, 1, 2, 3, 4, 5, 6	+/-1.0, +/-0.6, +/-0.2, +/-0.1, 0, 1.5

BLADED is a time domain aero-servo-elastic simulator that is used to conduct the high-fidelity aero-servo-elastic simulations of the same turbine geometry. The structural dynamics within BLADED are based on a modal model. The blade is modelled using up to 12 modes, six blade-flap and six blade-edge per blade. It also has three fore-aft and three side-to-side tower bending modes. Sophisticated power train dynamics are included. The aerodynamic model is based on the Blade Element Momentum theory. A design of experiments is produced as shown in Table 2. For each combina-

tion of wind speed, turbulence level and shear exponent we generate realizations of wind time series with 12 stochastic seeds. Some of the wind speed, turbulence and shear exponent combinations are excluded because they are unphysical, resulting in a total of 4344 10-minute simulations. One 10-minute wind time series simulation in BLADED takes approximately 25 minutes in real time. The output used from the simulations are the blade root flapwise bending moment. The global maxima of the bending moment data are extracted for each of the 4344 10-minute time series. The simulations in BLADED and FAST consider a wind turbine that has a 110 meters rotor diameter and 2 MW rated power. The wind turbine is erected on a 90 meters tower. Both the FAST and BLADED aero-servo-elastic simulations were performed with exactly the same control systems in the form of an external DLL. The FAST and BLADED simulation models do not use exactly the same input parameters in the structural and aerodynamic sub-models.

Table 2: Design of experiments for the BLADED simulations. The variables are wind speed [m/s], turbulence [m/s] and the wind shear exponent.

Wind Speed [m/s]	Turbulence [m/s]	Shear exponent [-]
4, 8, 10, 12, 15, 20, 25	0.1, 1, 2, 3, 4, 5, 6	+/-1.0,+/-0.6,+/-0.2,+/-0.1,0,1.5

5. RESULTS AND DISCUSSIONS

We start with a simple generic example to demonstrate Kriging and co-Kriging. In Figure 2, the noisy response of the low-fidelity simulator is plotted as a function of wind speed. A Universal Kriging model is fitted to the noisy response using a Gaussian correlation function R and a 3^{rd}-order polynomial basis. The low-fidelity Kriging model is then used as the trend to fit a co-Kriging model to the noisy high-fidelity response.

In Figure 3, we compare the co-Kriging model to a universal Kriging model (Gaussian correlation function R and a 2^{nd}-order polynomial basis).

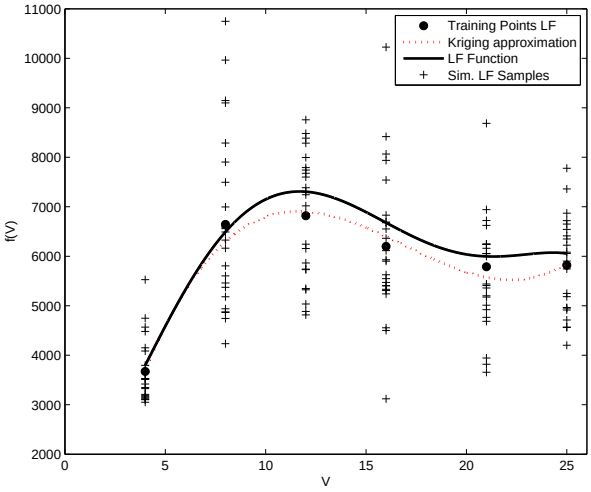

Figure 2: Response of the low-fidelity simulator at 6 wind speeds with 24 stochastic repetitions each (black crosses). The mean of the 24 samples is calculated and represented by the black dots. The Kriging model with noisy observations is the dotted red line. The low-fidelity (LF) function is the response if a large number of stochastic simulations are performed.

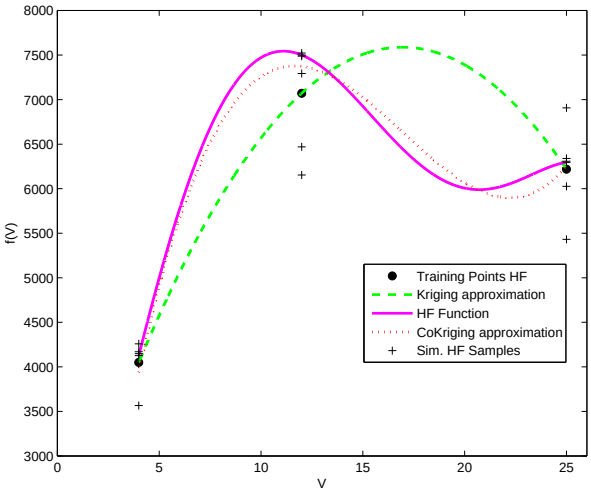

Figure 3: Response of the high-fidelity simulator at 3 wind speeds with 6 stochastic repetitions each (black crosses). The mean of the 6 samples is calculated and represented by the black dots. The Kriging model with noisy observations is the dashed green line. The Co-Kriging model with noisy observations is the dotted red line. The high-fidelity (HF) function is the response if a large number of stochastic simulations are performed.

Note that the high-fidelity responses are placed at only three wind speeds (4 m/s: turbine starts, 25 m/s: turbine shuts-down and 12 m/s: peak ro-

tor aerodynamic thrust). The co-Kriging predictions of the noisy high-fidelity response are notably better than the Kriging prediction based only on the high-fidelity samples. UQLab (Marelli and Sudret, 2014) is used to compute the Kriging and co-Kriging meta-models.

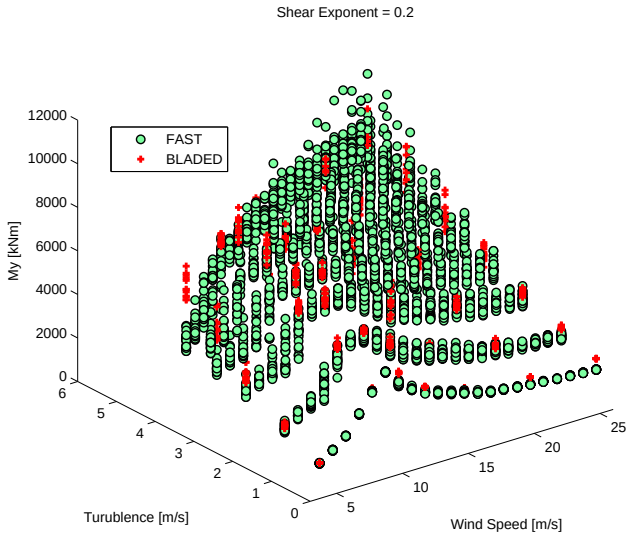

Figure 4: Scatter plot of the blade root extreme flapwise bending moment M_y as a function of wind speed and turbulence for shear exponent $\alpha = 0.2$. Note the variability (noise) of M_y for a given turbulence and wind speed.

A common practice during the design and optimization of a wind turbine is to generate a significant number of stochastic simulations, typically using two or more aero-servo-elastic simulators. Next, we show an example where the entirety of the loads simulations (as described in Section 4) are used to demonstrate a "real world" engineering application of data fusion using co-Kriging in high dimensions. The FAST and BLADED simulators were prepared by two independent engineers (one of whom is the first author of this paper). The simulations output are shown in Figure 4; even though the magnitude of the extreme flapwise bending moment at the blade root for low and high-fidelity simulators are not the same, they yield a similar trend. In Figure 4, for the same pair of turbulence and wind speed the output of the simulations is noisy due to the stochastic nature of the simulated wind speed time series. In addition, the magnitude of scatter (noise) increases with increasing turbulence level. Note that the low and high-fidelity simulators are not sampled at exactly the same input variables.

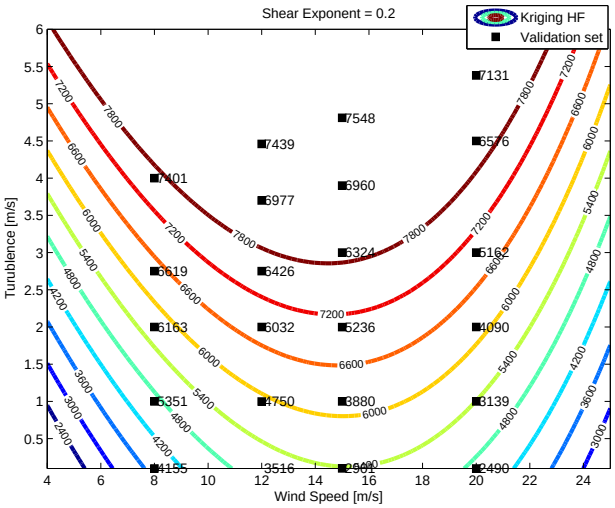

Figure 5: Projection of the Kriging model of the noisy high-fidelity (Bladed) extreme flapwise bending moment M_y compared to a validation set at wind speeds $V = 8, 12, 15, 20 m/s$ and shear $\alpha = 0.2$.

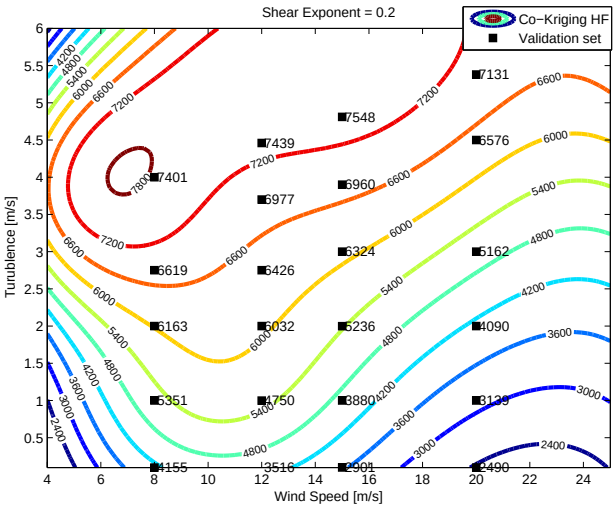

Figure 6: Projection of the Co-Kriging model of the of the noisy high-fidelity (Bladed) extreme flapwise bending moment M_y compared to a validation set at wind speeds $V = 8, 12, 15, 20 m/s$ and shear $\alpha = 0.2$.

A Universal Kriging model is first fitted to all the noisy load response of the low-fidelity simulator (FAST) using a Gaussian correlation function R and 3^{rd}-order polynomial basis. The low-fidelity Kriging model is then used as a model trend to fit a co-Kriging model to the noisy high-fidelity (Bladed)

load response. A subset of the high-fidelity data is used to build the co-Kriging model while the remaining data is used as validation points. This subset corresponds to the load response at wind speeds $V = [4, 10, 25]\, m/s$ as depicted in Figure 4. A universal Kriging model is also fitted to the same subset of the noisy high-fidelity load response using a Gaussian correlation function R and 2^{nd}-order polynomial basis. A projection of the Kriging and co-Kriging models of the noisy high-fidelity load response together with validation points are shown in Figures 5 and 6, respectively. To allow visualization of the meta-models predictions we set the shear exponent to $\alpha = 0.2$. Qualitatively, one can see that the co-Kriging model predictions are close to the validation points, while the Kriging model generally over-predicts the extreme load response. Using the low-fidelity Kriging model as a trend improves the predictive accuracy of the co-Kriging model of the high-fidelity load response, even in the presence of noise and by using very few high-fidelity sample points.

This is shown more clearly in Figures 7–9 where the accuracy of the Kriging and co-Kriging models of the high-fidelity extreme load response are compared. In those figures the validation points are shown with the corresponding scatter. The Kriging model from the high-fidelity response points gives a poor approximation of the validation points, while the co-Kriging model performs notably better in high dimensions. Hence, despite the difference between the output of the low and high-fidelity simulators, we were able to fuse both data sets so that the prediction error of the high-fidelity load response is reduced. The 95% confidence interval of the co-Kriging predictions is also shown in Figures 7, 8 and 9. The confidence interval of the co-Kriging predictions reflects a mix of epistemic (statistical) uncertainty due to the number of sampled points and due to the noise in the simulations output.

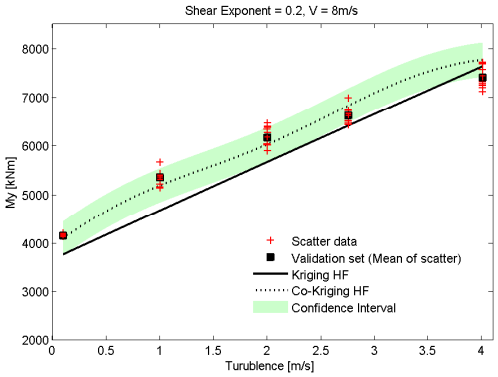

Figure 7: Comparison of the Kriging and co-Kriging models of the high-fidelity (HF) extreme flapwise bending moment M_y as a function of turbulence for $\alpha = 0.2$ and $V = 8m/s$.

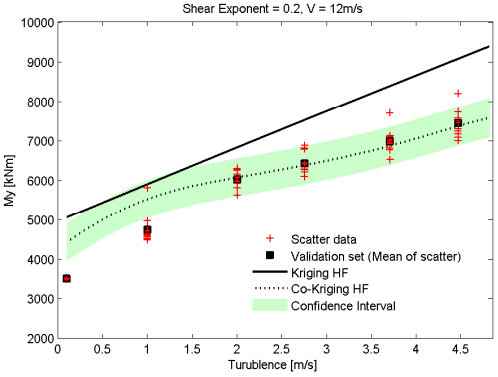

Figure 8: Comparison of the Kriging and co-Kriging models of the high-fidelity (HF) extreme flapwise bending moment M_y as a function of turbulence for $\alpha = 0.2$ and $V = 12m/s$.

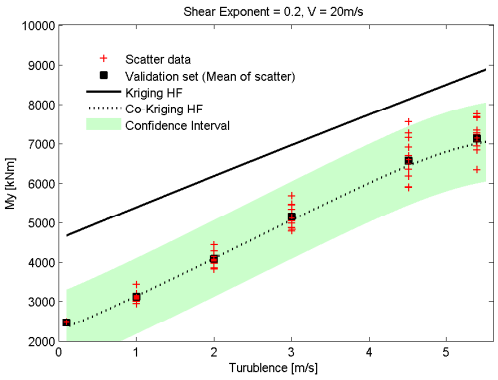

Figure 9: Comparison of the Kriging and co-Kriging models of the high-fidelity (HF) extreme flapwise bending moment M_y as a function of turbulence for $\alpha = 0.2$ and $V = 20m/s$.

6. CONCLUSIONS

We have shown a co-Kriging based methodology to fuse the "noisy" extreme flapwise bending moment at the blade root of a large wind turbine from a low-fidelity and a high-fidelity aero-servo-elastic simulator. With limited high-fidelity response samples, the co-Kriging predictions compared well with val-

idation data. The notably accurate prediction performance is due to using the low-fidelity Kriging model as a model trend for the co-Kriging model. It is straight forward to extend this method to multiple fidelity levels. The confidence interval on the predictions of the co-Kriging model reflects a mix of epistemic (statistical) uncertainty due to the number of sampled points and due to the noise in the simulations output. A future study could attempt to quantify these two sources of uncertainties separately. In this paper, the main assumption is that the high and low-fidelity aero-servo-elastic simulations follow similar trends, which makes the fusion of results feasible. If the trend were not present then fusing data using co-Kriging would become hard to perform and less reliable. Finally, extreme loads response of a wind turbine are known not to follow a Gaussian process; a future study could attempt to modify the co-Kriging methodology to include non-Gaussian processes.

7. REFERENCES

Bachoc, F. (2013). "Cross validation and maximum likelihood estimations of hyper-parameters of Gaussian processes with model misspecifications." *Comput. Stat. Data Anal.*, 66, 55–69.

Bossanyi, E. (2003a). "GH Bladed theory manual." *Report No. 282-BR-009*, DNV GL.

Bossanyi, E. (2003b). "GH Bladed user manual." *Report No. 282-BR-010*, DNV GL.

Christensen, D. E. (2012). "Multifidelity methods for multidisciplinary design under uncertainty." M.S. thesis, Massachusetts Institute of Technology, Departement of aeronautics and astronautics.

Dubourg, V. (2011). "Adaptive surrogate models for reliability analysis and reliability-based design optimization." Ph.D. thesis, Université Blaise Pascal - Clermont II, LaMI.

Forrester, A. I., Sóbester, A., and Keane, A. J. (2007). "Multi-fidelity optimization via surrogate modelling." *Proceedings of the Royal Society A: Mathematical, Physical and Engineering Sciences*, 463(2088), 3251–3269.

Han, Z., Zimmerman, R., and Görtz, S. (2012). "Alternative cokriging method for variable-fidelity surrogate modeling." *AIAA Journal*, 50(5), 1205–1210.

Han, Z.-H. and Görtz, S. (2012). "Hierarchical Kriging model for variable-fidelity surrogate modeling." *AIAA Journal*, 50(9), 1885–1896.

Hansen, M. (2001). *Aerodynamics of wind turbines : rotors, loads and structure*. James & James (Science Publishers) Ltd. pp. 152. ISBN 1902916069.

Jones, D. R. (2001). "A Taxonomy of global optimization methods Based on response surfaces." *Journal of Global Optimization*, 345–383.

Jonkman, J. and Buhl, M. (2005). "FAST user's guide." *Report No. NREL/EL-500-38230*, National Renewable Energy Laboratory.

Kennedy, M. and O'Hagan, A. (2000). "Predicting the output from a complex computer code when fast approximations are available." *Biometrika*, 87(1), 1–13.

Marelli, S. and Sudret, B. (2014). "UQLab: a framework for uncertainty quantification in MATLAB." *Proc. 2nd Int. Conf. on Vulnerability, Risk Analysis and Management (ICVRAM2014), Liverpool, United Kingdom*.

Picheny, V., Wagner, T., and Ginsbourger, D. (2012). "A benchmark of kriging-based infill criteria for noisy optimization.

Sacks, J., Welch, W., Mitchell, T., and Wynn, H. (1989). "Design and analysis of computer experiments." *Stat. Sci.*, 4, 409–435.

Schöbi, R. and Sudret, B. (2014). "Polynomial-chaos-based kriging." *Int. J. Uncertainty Quantification,* submitted.

Sudret, B. (2012). "Meta-models for structural reliability and uncertainty quantification." *Fifth Asian-Pacific Symposium on Structural Reliability and its Applications*, <http://arxiv.org/abs/1203.2062>.